مجلة جمعية الليزر العراقية
Iraqi Laser Society Journal
I.L.S.J.
Issue-2 1st Year 2024

CuOFe2O3, MnOFe2O3 and ZnOFe2O3 -Curcumin Nanocomposites: Hydrothermal Method Synthesis, Characterization, and Antimicrobial Studies

Malik Jafar Rabee[1], Basim Ibrahim Al-Abdaly[2] and Mustafa M. Kadhim[3]

[1] Department of Chemistry/ College of Science/ University of Misan/Misan/ Iraq,

[2] Department of Chemistry/ College of Science/ University of Baghdad/Baghdad/ Iraq

email: basim.ibrahim@sc.uobaghdad.edu.iq

[3] Department of chemical and oil refining engineering/ Kut University College /Wasit / Iraq

Abstract

This paper presents the synthesis of nanocurcumin with some spinel oxides (CuOFe2O3, MnOFe2O3, ZnOFe2O3) as nanocomposites by hydrothermal method. Synthesized nanocomposites were characterized by using various techniques: Fourier transformed infrared spectroscopy (FT-IR), energy-dispersive X-ray spectroscopy (EDS), X-ray diffraction (XRD). The morphology of the surface was evaluated by scanning electron microscope (SEM), and atomic electron microscope (AFM). XRD has been demonstrated success in forming spinel oxide with cubic crystallites phase, and the mean particle size calculated by the Debye-Scherrer formula (22.8-17.7 nm). Curcumin nanocomposites display high efficacy against microbes and were the greatest for [CuOFe2O3/curcumin] nanocomposite.

Keywords: Metal Oxides/Curcumin, Precursor, Nanocomposites, Autoclave, and Antibacterial

مجلة جمعية الليزر العراقية
Iraqi Laser Society Journal
I.L.S.J.
Issue-2 1st Year 2024

تخليق مركبات الكركمين النانوية: CuOFe2O3, Mgofe2o3 و ZnO Fe2O3 - الطريقة الحرارية المائية والتوصيف ودراسات مضادات الميكروبات

مالك جعفر ربيع [1] ، باسم إبراهيم العبدلي [2] ، مصطفى محمد كاظم [3]

قسم الكيمياء / كلية العلوم / جامعة ميسان / ميسان / العراق 1,

قسم الكيمياء / كلية العلوم / جامعة بغداد / بغداد / العراق 2

email: basim.ibrahim@sc.uobaghdad.edu.iq

قسم هندسة الكيماويات وتكرير النفط / كلية الكوت الجامعية / واسط / العراق 3

الخلاصة

الغرض من الدراسة هو تقييم مستوى القلق والاكتئاب لدى طلاب المرحلة المتوسطة. وتحديد الارتباط بخصائصهم مثل عمر الطلاب والجنس والدرجة الدراسية في مدينة الناصرية / العراق. طرق البحث: أجريت دراسة وصفية على 492 طالباً وطالبة تم اختيارهم بطريقة عشوائية بسيطة من 6 مدارس متوسطة في مدينة الناصرية. تم إثبات موثوقية الاستبيان من خلال دراسة تجريبية، وتم تقديمه لاحقًا إلى الخبراء للتحقق من صحته. تم جمع المعلومات من خلال استخدام تقنيات التقرير الذاتي وتحليلها من خلال تطبيق التحليل الإحصائي الوصفي والاستدلالي. النتائج: العمر 13 و 14 سنة ولكل منهما (33.5%)، كانت الغلبة للطالبات بنسبة (58.3%)، وسجل طلاب المرحلة الأولى أعلى نسبة (37.2%)، وأبدى (49%) من الطلاب أ مستوى مرتفع من القلق، وأعرب أغلبية (65%) عن مستوى متوسط من الاكتئاب. وكانت هناك فروق ذات دلالة إحصائية في مستوى القلق بين الجنسين.($P = 0.022$) الاستنتاج: أبدى طلاب المدارس المتوسطة مستوى مرتفع من القلق ومستوى متوسط من الاكتئاب بسبب نقص برامج الصحة النفسية المدرسية، واختلاف مستوى القلق باختلاف جنس الطلاب. يجب إنشاء استشارات الصحة العقلية في المدارس وتوفير مستشارين محترفين لمنع القلق الخطير لدى الطلاب والحاجة إلى تقليل الضغط الأكاديمي للطلاب. يجب على الآباء أن يكونوا أكثر وعياً بالحالة النفسية لأطفالهم خاصة خلال فترة المراهقة حيث أن انتشار الاضطراب النفسي يتزايد بشكل ملحوظ مع مرور الوقت.

الكلمات المفتاحية: أكاسيد المعادن / الكركمين ، السلائف ، المركبات النانوية ، الأوتوكلاف ، ومضاد للبكتيريا

Introduction:

Curcumin, an active. component mainly derived from Curcuma longa (turmeric), is a natural yellow-orange polyphenol, it has a long history of being administered by various people in China, India and Iran for the treatment of many diseases such as diabetes, liver disease, rheumatoid diseases, arteriosclerosis, infectious diseases, cancers and disorders. [1, 2]. Many researchers have worked on curcumin due to its different therapeutic effects on different diseases. Soon after, curcumin received attention mostly due to its antioxidant, anti-inflammatory, anti-tumor, inducing apoptosis, and anti-angiogenic, which has been reported in several investigations. It acts on multiple targets in the cellular pathways making this agent capable of performing multiple actions [3–7]. Nanotechnology is increasingly the technology of the future. Among the wide applications of nanotechnology is the use of nanoparticles to enhance the bioavailability and solubility of lipophilic compounds such as curcumin in drug delivery systems. Therefore, the application of nanoparticles has gained immense popularity in the past decade due to their ability to improve the therapeutic effects of coated drugs by protecting drugs from enzymatic hydrolysis, altering their pharmacokinetics, reducing their toxicity, and reducing their nonspecific assimilation [8,9]. Over a period of time, emphasis has been placed on developing natural curcumin biodistribution, but only recently the application of the field of nanotechnology has greatly enhanced its therapeutic effects. Nanoparticles such as nanoparticles, polymeric nanoparticles, micelles, nanoparticles, nanosomes, cyclodextrin, dendrites, silver, and solid lipids are emerging as one of the beneficial alternatives that have been shown to offer therapeutic concentrations of curcumin. The use of the nanoparticles mentioned above has improved major problems of curcumin such as reduced solubility, instability, impaired bioavailability, rapid metabolism in carcinomas, wound healing, Alzheimer's disease, epilepsy, ischemia and inflammatory diseases [10-12]. It is for these reasons that were prepared the spinel oxides CuOFe2O3, MnOFe2O3, and ZnOFe2O3 with nanocurcumin as nanocomposites to enhance curcumin solubility in aqueous solutions and efficacy as a drug, by preparing it via the hydrothermal method and testing its bioavailability against a number of bacteria. Nanocomposites vary from the conventional composite materials because of the remarkably higher surface to volume ratio of the reinforcing phase and/or extremely higher characteristic ratio, increased ductility with no decrease of strength and scratching resistance. Recent years, various varieties of nanocomposites such as inorganic-inorganic, organic-inorganic, and organic-organic nanocomposites have been manufactured and evaluated for variety of industrial applications in numerous areas, such as antimicrobial, biomedical, pharmaceutical, packaging, coating, electronics, and aerospace industries.

1.Experimental

1.1. Materials and methods

Curcumin C21H20O6 (368.38g/mol, Himedia), Copper (II) acetate monohydrate Cu (CH3COO)2.H2O (199.65 g/mol, sigma alrich), Zinc acetate dihydrate Zn (CH3COO)2.2H2O (219.50 g/mol, Fluka), Manganese acetate dihydrate Mn(CH3COO)2.2H2O (209.055 g/mol,) and Iron (III) chloride dihydrate FeCl3.2H2O (162.204 g/mol, CDH).

1.2. Instrumental

Measurements of Fourier transform Infrared spectroscopy (FT-IR) was conducted in the Department of Chemistry/ College of science/ University of

Baghdad/Iraq using SHIMADZU FT-IR 8400S/Japan.

Measurements of X-ray diffraction (XRD) were conducted in XRD University of Kashan\ Iran using SHIMADZU (XRD) 6000 X-Ray Target Cu K/ α radiation (λ=1.54180Å)/ JAPAN. Measurements of Energy Dispersive X-ray spectroscopy (EDS or EDX) and Scanning Electron microscope (SEM) were conducted in University of Kashan / Iran. Atomic force microscope /(AFM) was conducted in Chemistry Department, College of Science, University of Baghdad Model AA3000/ Angstrom Advanced Inc/USA.

1.3. Synthesis of [curcumin/ ZnO:Fe2O3] nanocomposite.

Weigh 0.8g (0.004 mol) from FeCl3.2H2O and 0.43g (0.004 mol) of Zn(CH3COO)2.2H2O dissolved in 40 ml of deionized water with stirring for 30 min. Wight a 1g of curcumin add in 35 ml of deionized water with stirring for 30 min. Tow solutions mixed with stirring for 1h. Then the dispersion was transferred into Teflon lined stainless autoclave at (150–180) °C for (6–24) h. Different parameters such as time, temperature were studied. The optimum conditions were 24 h and 180 °C (the heating rate = 2 °C /min). The cell was cooled, and its contents have been separated by centrifugation (4000 rpm). The separated brown-black was washed by distilled water four times and dried in an oven at 60 °C for 12 h.

1.4. Synthesis of [curcumin/ CuO:Fe2O3] nanocomposite.

Weigh 0.8g (0.004 mol) from FeCl3.2H2O and 0.4g (0.002 mol) of Cu(CH3COO)2.H2O dissolved in 40 ml of deionized water with stirring for 30 min. Wight a 1g of curcumin add in 35 ml of deionized water with stirring for 30 min., then added the second solution to the first solution prepared above and continuous stirring for 1h. The resulted solution was transferred into Teflon lined stainless autoclave at 150 °C for 24 h, heating rate = 2 °C

/min. The cell was cooled, and its contents have been separated by centrifugation (4000 rpm). The separated brown black was washed by distilled water four times and dried in an oven at 60 °C for 12h.

1.5. Synthesis of [curcumin/ MnO: Fe2O3] nanocomposite.

Weigh 0.8g (0.004mol) from $FeCl_3.2H_2O$ and 0.49g (0.002 mol) of $Mn(CH_3COO)_2.2H_2O$ dissolved in 40 ml of deionized water with stirring for 30 min. Wight a 1g of curcumin add in 35 ml of deionized water with stirring for 30 min., then added the second solution to the first solution prepared above and continuous stirring for 1h. Then the solution was transferred into Teflon lined stainless autoclave at 180 °C for 24 h, heating rate = 2 °C /min. The cell was cooled, and its contents have been separated by centrifugation (4000 rpm). The separated brown black was washed by distilled water four times and dried in an oven at 60 °C for 12 h.

2. Characterization

The images and their results of AFM for curcumin nanostructure and its nanocomposites synthesized were shown in figure (1). It is noted for nanocurcumin structure, the grooves are not homogenous as showed by three-dimensional image, which is mainly due to agglomeration nanoparticles of the curcumin surface and showed that the diameter of the particle was in average of 71.0 nm figure(1a). For [ZnOFe2O3 /curcumin] nanocomposite figure (1b), the grooves are not homogenous also as depicted by three-dimensional image, which is mainly due to agglomeration of oxides nanoparticles which coating of curcumin surface nanoparticles and showed that the diameter of the particle was in average of 70.71 nm, for [MnOFe2O3/ curcumin] nanostructure figure (1c) was shown the average diameter to be 68.17 nm, and for [CuOFe2O3/ curcumin] nanostructure figure (1d) showed that the diameter of the particles was in average 70.71nm.

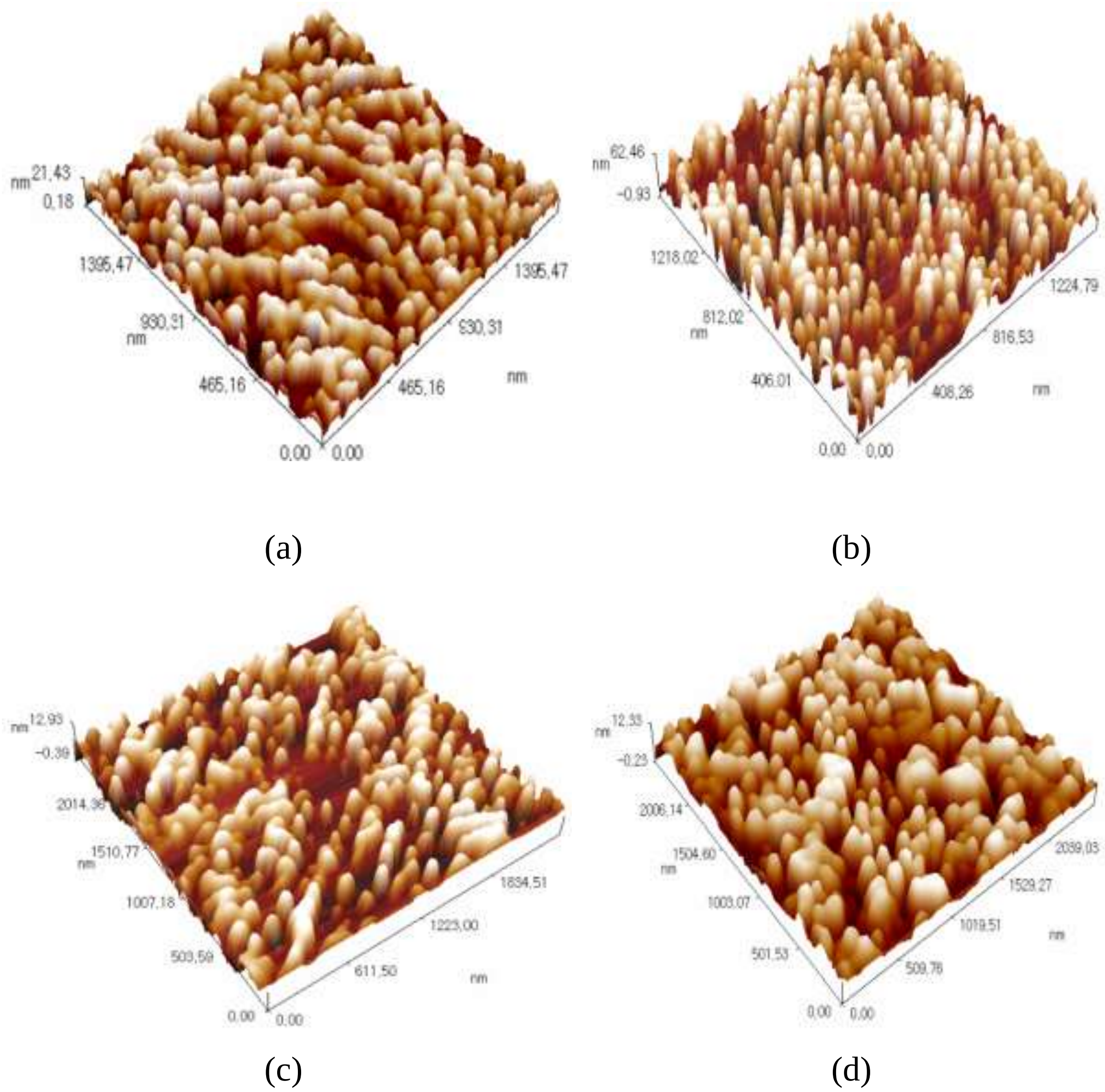

Fig (1): (3D) AFM images of (a) Nanocurcumin. (b)[ZnOFe2O3/ curcumin] nanocomposite. (c) [MnOFe2O3/ curcumin] nanocomposite. (d) [CuOFe2O3/ curcumin] nanocomposite.

2.1. Analysis of (FT-IR) spectral data for nanocurcumin composites

Infrared spectra give the most information about the compounds structure. The FTIR spectra of curcumin produced a characteristic stretching band of OH at 3512.13 cm-1 figure (3.27). The peak at 3014 cm-1 pertains to C–H stretching, and 1600.09 cm-1 peak represents C=C symmetric aromatic ring stretching. The peak at 1512.06 cm-1 is for

C=O, while enol C–O aromatic peak was seen at 1280.65 cm-1 and benzoate trans-C–H vibration could be observed at 964.34 cm-1, and peak refer to methoxy group (O_CH3) at 1029.92 cm-1 [13,14]. No peak was observed in the carbonyl region (1800–1650 cm-1), suggesting that curcumin existed in the keto-enol tautomeric formula [15].

The FTIR spectra of all nanocomposites synthesized compared to the pure NCur all characteristic peaks were observed to shift lower or high wavenumber. The FT-IR spectrum of [ZnOFe2O3/curcumin] nanocomposite is reported in figure (3). The broad bands at (3386.77,1514.06, and 1272.95) cm-1 are indicated to the stretching vibrations of (O-H), (C=O) and C-O groups respectively. The band at 2966 cm-1 is attributed to the stretching vibration of (C–H). The bands from 435 cm-1 to 800 cm-1 indicate to metal oxides M-O, the band at 428 cm-1 is due to the vibration of Fe-O bond at octahedron position and the band at 546 cm-1 is obtained due to the vibration of Zn-O bond at position of the tetrahedron, respectively [16].

The FT-IR spectrum of [MnOFe2O3/curcumin] nanocomposite shown in figure (4). The bands at 3396.41cm-1 and 1691.46 cm-1 are related to O–H and C=O groups, respectively. Absorption at 2972 cm-1 is related to C–H bonds. Peak at 1600 cm-1 is refer to C=C and peak at 1269 cm-1 is attributed to the stretching vibration of C-O group. Two peaks at 561 and 430 cm-1 were attributed to the intrinsic stretching vibrations of tetrahedral sites Mn-O and octahedral sites of Fe-O structures, respectively [17].

The FT-IR spectrum of [CuOFe2O3/curcumin] nanocomposite shown in figure (5). The broad bands at 3494.77 cm-1 is refer to the stretching vibrations of O–H group. The bands at 1695.3

cm-1and the strong band at1598.88 cm-1 are related to C=O and C=C groups respectively, broad peak at 1271 cm-1 is attributed to the stretching vibration of C-O group. The absorption peaks were observed in the range of 619, 578.6 cm-1 and 422.3-486 cm-1, these bands are attributed to the vibration of Cu-O and Fe-O respectively [18].

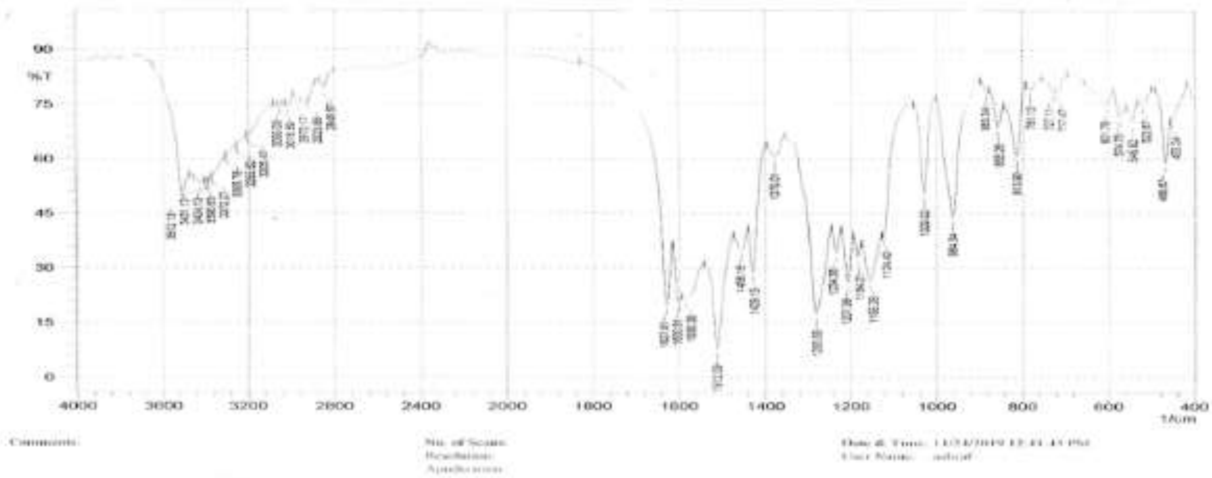

Fig (2): FT-IR spectrum of nanocurcumin (NCur).

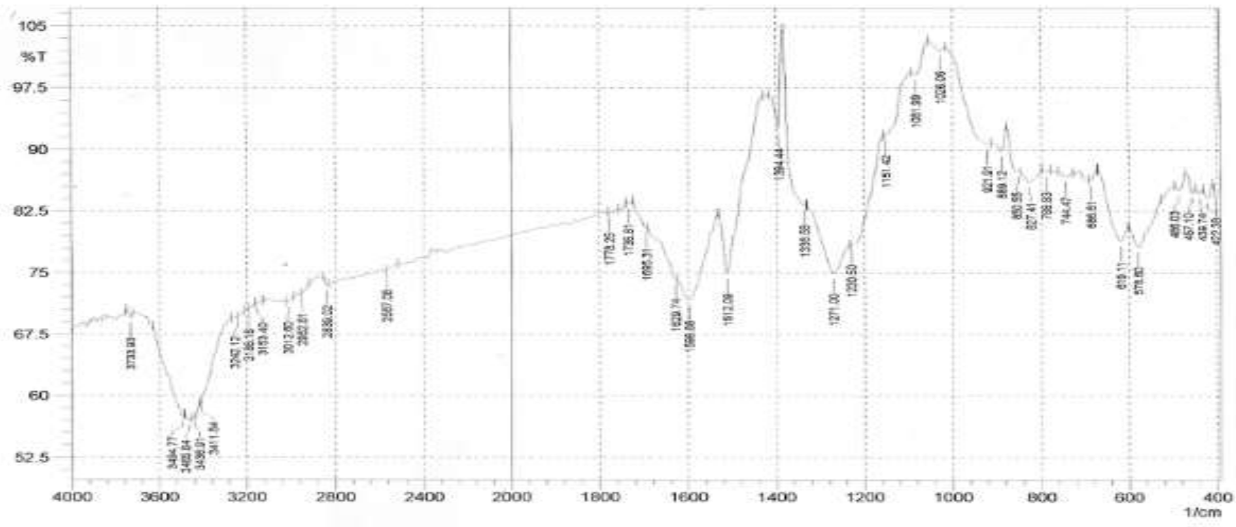

Fig (3): FT-IR spectrum of [CuOFe2O3 / curcumin] nano composite.

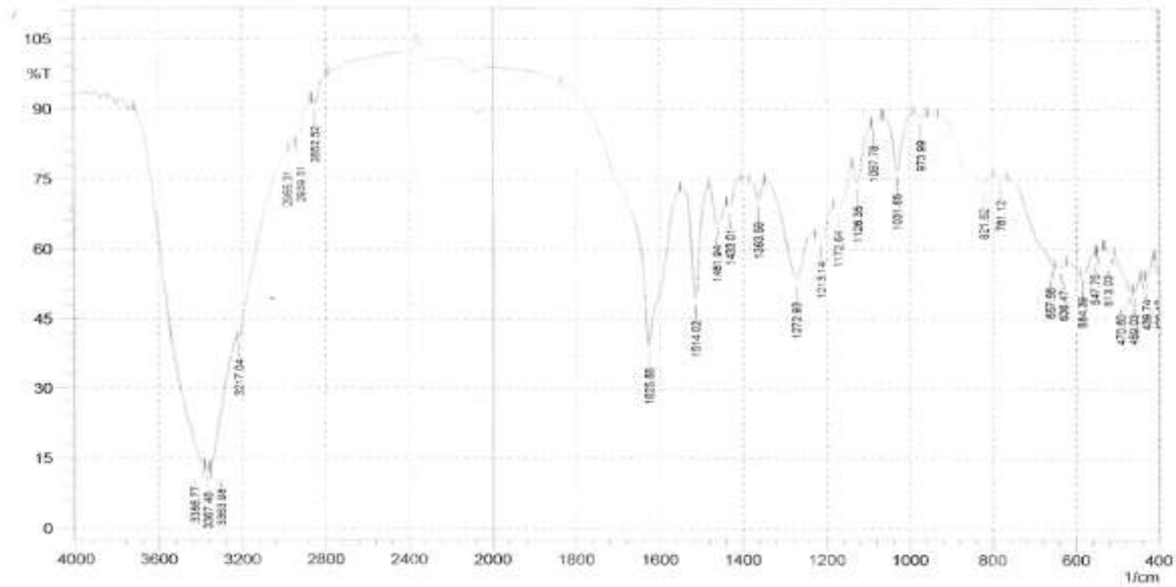

Fig (4): FT-IR spectrum of [ZnOFe2O3/ curcumin] nano composite

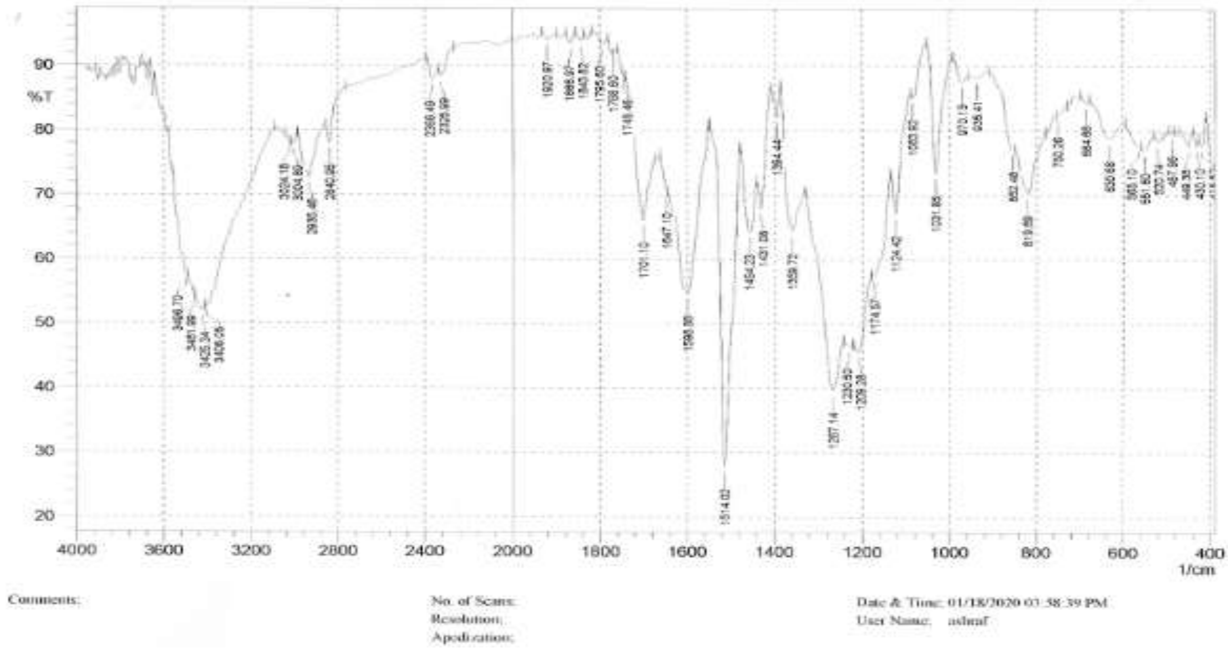

Fig (5): FT-IR spectrum of [MnOFe2O3 /curcumin] nanocomposite

2.2. Surface morphology analysis via SEM and EDS

The morphology, particle size distribution and the percentage of the components of curcumin and its nanocomposites were investigated by SEM, EDX techniques. As shown in figure (6-A), the SEM image for nanocurcumin showed of surface morphology contains kinds of spherical particles, the EDX spectrum showed a peak for carbon 62.26% and oxygen 38.74%, figure(7-A). The SEM image for [CuOFe2O3 / curcumin] showed that the sample contains kinds of particles spherical with morphology such as cluster as shown in figure (6-B) [19]. Also, EDX spectrum rise in peak intensity of copper with 5.27%, 40.40% of oxygen, 11.65% ferrite and carbon 42.68%, figure(7-B). The [ZnOFe2O3/ curcumin] composite showed along with mapping its components figure (6-C). The SEM for [ZnOFe2O3 /curcumin] showed the nano-granular morphology created by the aggregation of little globular structures where it formed in the form of balls and tubes figure, the EDX spectrum showed a peak for zinc 0.75%, ferrite 1.05%, carbon 62.31% and oxygen 35.9%, figure(7-C). The [MnOFe2O3 / curcumin] composite showed along with mapping its components figure (6-D). The SEM for [MnOFe2O3 / curcumin] showed coatings have a globular shape and nonhomogeneous spherical morphology. The EDX spectrum showed a peak for manganese 1.06%, ferrite 1.88%, carbon 59.80% and oxygen 37.26%,figure(7-D).

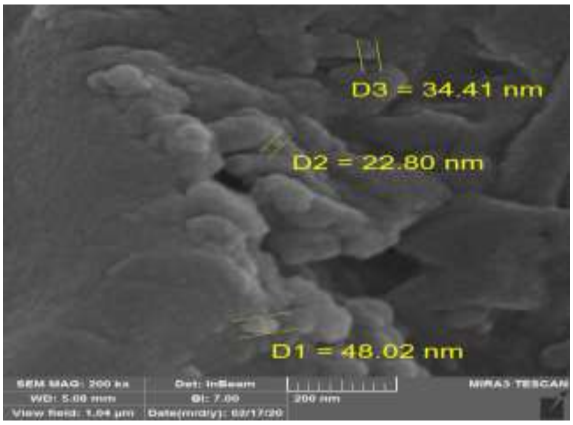

(a)

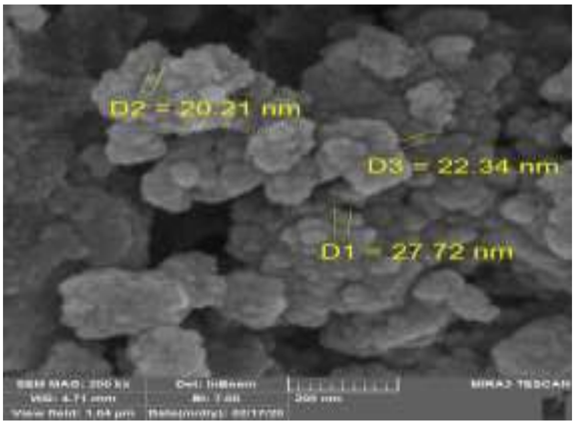

(b)

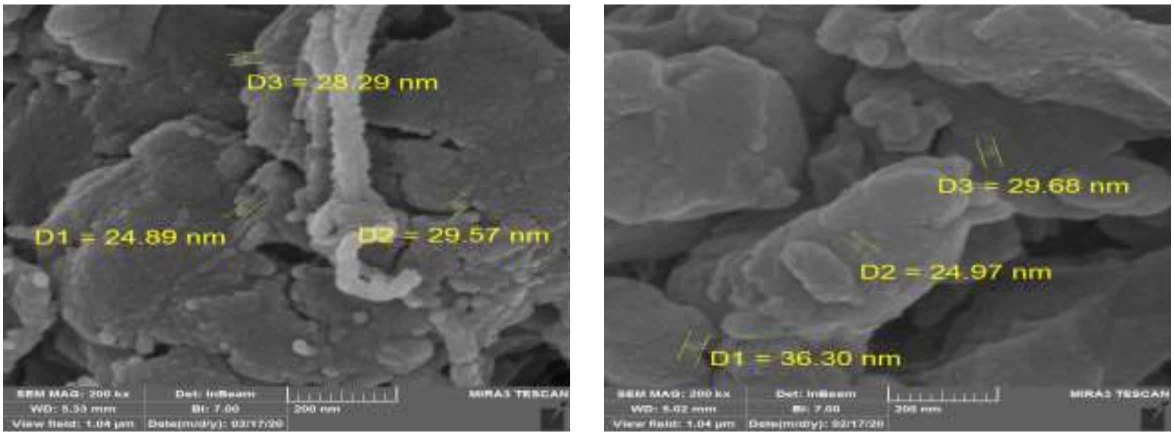

(c) (d)

Fig (6): SEM images for (a) nanocurcumin. (b) [CuOFe2O3 / curcumin] nanocomposite. (c) [ZnOFe2O3/ curcumin] nanocomposite. (d) [MnOFe2O3/ curcumin] nanocomposite

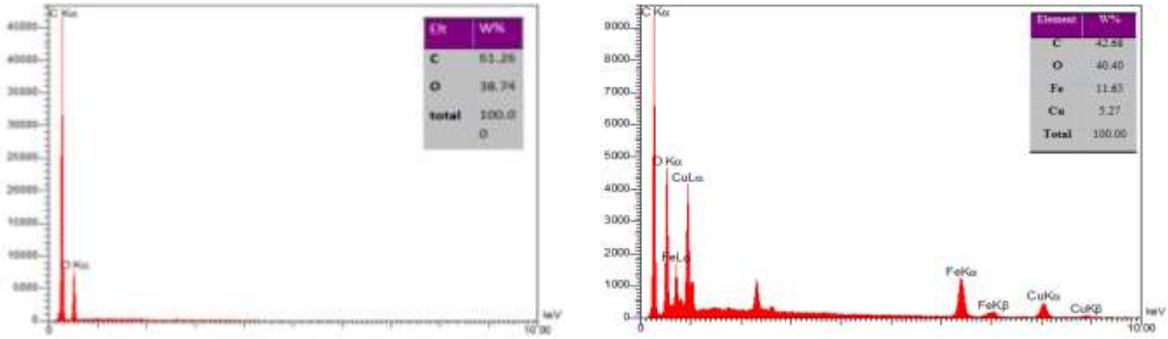

(a) (b)

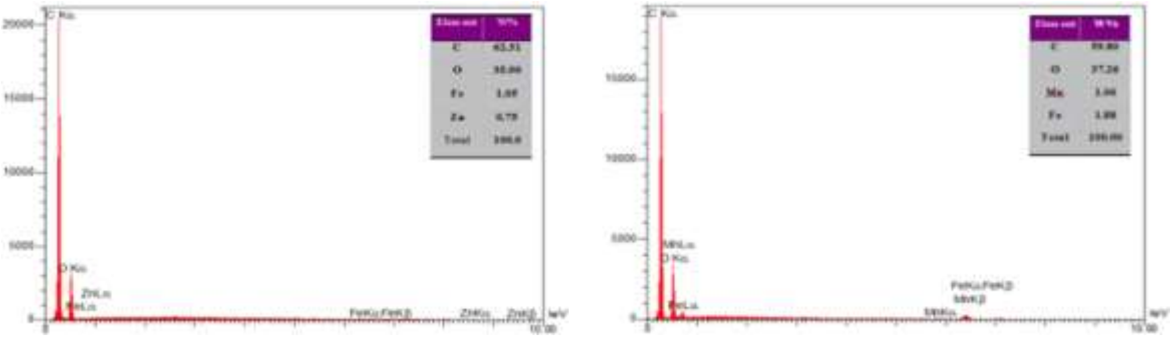

(c) (d)

Fig (7): EDS spectra of (a) nanocurcumin, (b) [CuOFe2O3 / curcumin] nanocomposite, (c) [ZnOFe2O3/ curcumin] nanocomposite, (d) [MnOFe2O3/ curcumin] nanocomposite

2.3. X-Ray diffraction of curcumin nanocomposites

The XRD pattern shows a significant amount of broadening lines which are characteristic of nanoparticles. The crystallite size can be calculated according to Debye-Scherrer formula [20]:

$$D= k\, \lambda\, /\beta COS\, \theta$$

Where k = 0.9 Scherrer constant, λ is the wavelength of the Cu-Kα radiation, β is the full width at half maximum and θ is the angle obtained from 2θ values corresponding to maximum intensity peak in XRD pattern.

The XRD pattern of [CuOFe2O3 / Cur] nanocomposite shown in figure (8). The peaks refer to CuOFe2O3 observed at 2θ = 36.4°, 43° and 62° which relate to the reflection planes (311), (400) and (440) respectively. Crystalline phase is a cubic [21-23]. Most of the peaks belonging to the CuOFe2O3 nanoparticles were shifted slightly to the higher angle indicating the stresses in the crystal lattice due to the lower average lattice parameters by the nanocurcumin particles. The main particle size of the [CuOFe2O3/Cur] nanocomposite approximately (22.8 nm) in diameter. The XRD pattern of [MnOFe2O3/Cur] nanocomposite shown in figure (9), the peaks are donated to MnOFe2O3 which observed diffraction peaks at the 2θ = 30.2°, 35.6°, 43.3°, 53.6°, 57° and 62.7°, which are matching to crystal planes of (220), (311), (400), (422), (511) and (440) respectively (JCPDS card No. 10-0319) [24,25]. The crystalline phase is cubic. The main particles size of the [MnOFe2O3/Cur] nanocomposite approximately (19.8 nm) in diameter. In figure (10) XRD pattern of [ZnOFe2O3 / Cur] nanocomposite, which shows semi-crystallite structures, the weak peak is donated to ZnOFe2O3 which observed diffraction peak at the 2θ = 35.8°, which are corresponding to crystal plane of (311) [26]. The peaks of ZnOFe2O3 disappeared with nanocomposite, which is likely caused by a change from crystalline form to amorphous form or even possible due distribute nanocurcumin crystals in a thin layer on the ZnOFe2O3 nanoparticles. The main particle size of the [ZnOFe2O3/Cur] nanocomposite approximately (17.7 nm) in diameter.

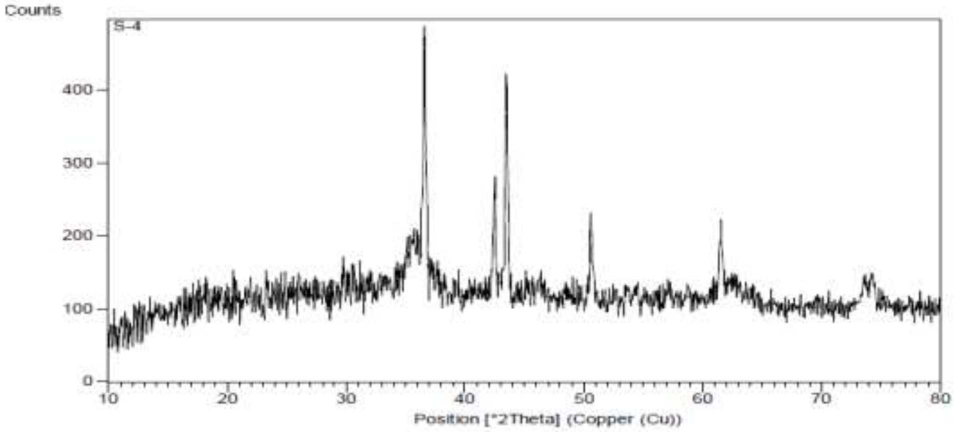

Fig (8): XRD Pattern of [CuOFe2O3 / curcumin] nanostructure

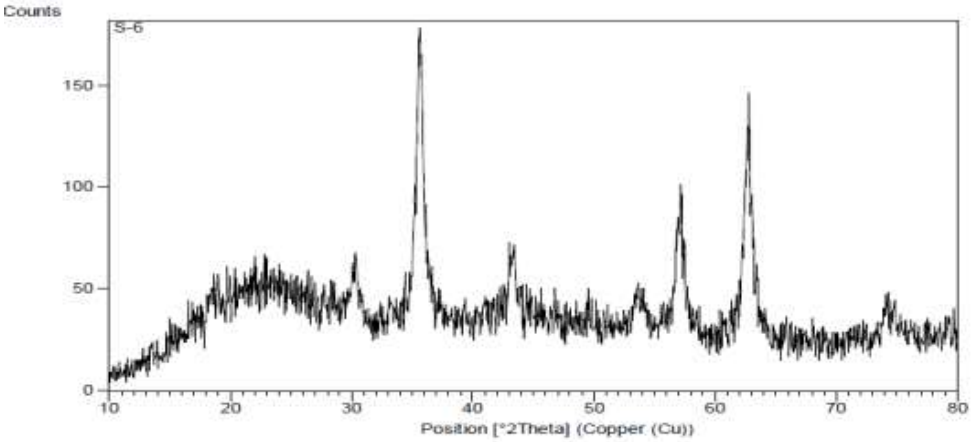

Fig (9): XRD Pattern of [MnOFe2O3/curcumin] nanostructure

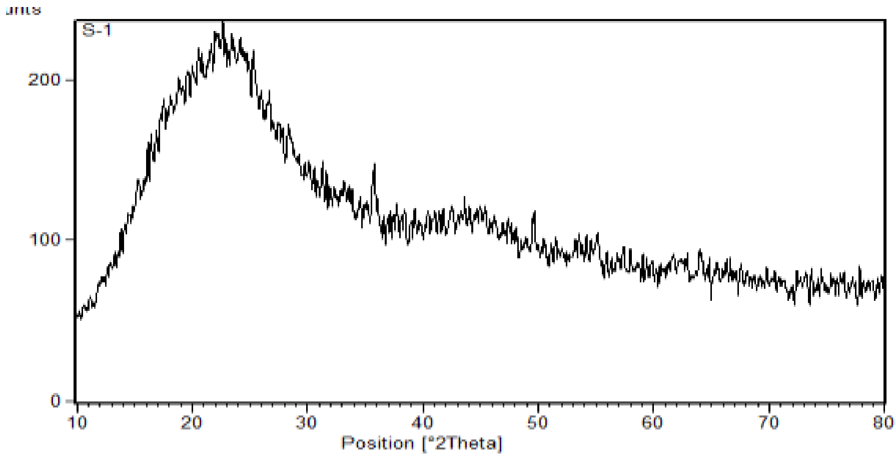

Fig (10): XRD Pattern of [ZnOFe2O3 / curcumin] nanostructure

3. Antibacterial activity of curcumin / spinel oxides nanocomposites

All prepared nanostructures as nanocomposites. Its biological activity has been tested against four bacteria [Escherichia Coli (-), Staphylococcus aureus (+), Bacillus cereus (+), Pseudomonas aeruginosa (-)] and exhibited an activity. It has been observed that the levels of antibacterial activities of nanocurcumin [NCur] at the highest concentration of nanoparticles was largest zone of inhibition (16mm) against (Pseudo), (E-coil) and (staph). The zone of inhibition in (15mm) was observed for [NCur] against (B. cereus) at the highest concentration of nanoparticles. The nanocurcumin aqueous diffusion had an antimicrobial influence stronger than the curcumin [7]. While levels of anti-bacterial activities are observed of the composites were different in an inhibition zone as shown in (Table 1). The largest zone of inhibition (40mm) was observed for [CuOFe2O3/curcumin] composite at the highest concentration against (E-coil) and the largest zone of inhibition (38mm) was observed for [CuOFe2O/3cucumin] composite against (Pseudo) and (staph) in the highest of concentration of nanoparticles. Also, the largest zone of inhibition (36mm) was observed for [CuOFe2O3/curcumin] composite against (B cereus). as shown in the figures (11). The effectiveness of the composites was as follows:

[NCur/CuOFe2O3] > [NCur/ZnOFe2O3] > [NCur/MnOFe2O3] with Escherichia Coli (-)

[NCur/ZnO Fe2O3] > [NCur/CuO Fe2O3] > [NCur/MnO Fe2O3] = Bacillus cereus (+)

[NCur/CuO Fe2O3] > [NCur/ZnO Fe2O3] > [NCur/MnO Fe2O3] = Pseudomonas aeruginosa (-).

[NCur/CuOFe2O3] > [NCur/ZnO Fe2O3] > [NCur/MnOFe2O3] = Staphylococcus aureus (+)

Curcumin and nanomeric curcumin have been shown to be effective against bacteria strains. The size of nanocurcumin is much less than the size of normal curcumin which enhances penetration and higher uptake by the cells [27,28]. In addition, loading some elements increases its effectiveness against bacteria.

Table (2): Inhibition of pathogenic bacteria on curcumin nanocomposites.

No.	***formula***	***Escherichia Coli (-)***	**Bacillus cereus (+)**	***Staphylococcus aureus (+)***	***pseudomonas aeruginosa (-)***
1	**NCur**	**16**	**15**	**16**	**16**
2	**NCur/MnO:Fe_2O_3**	**22**	**21**	**22**	**18**
3	**NCur/CuO:Fe_2O_3**	**40**	**36**	**38**	**38**
4	**NCur/ZnO:Fe_2O_3**	**24**	**31**	**27**	**28**

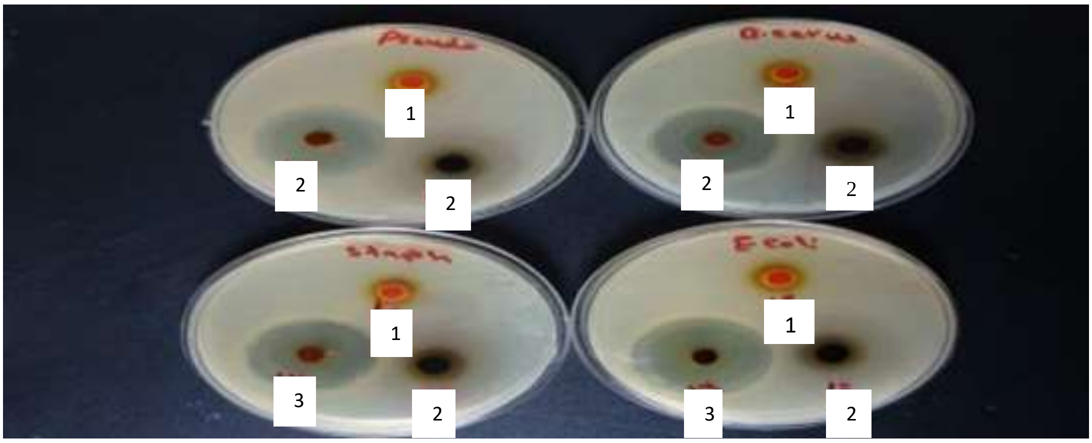

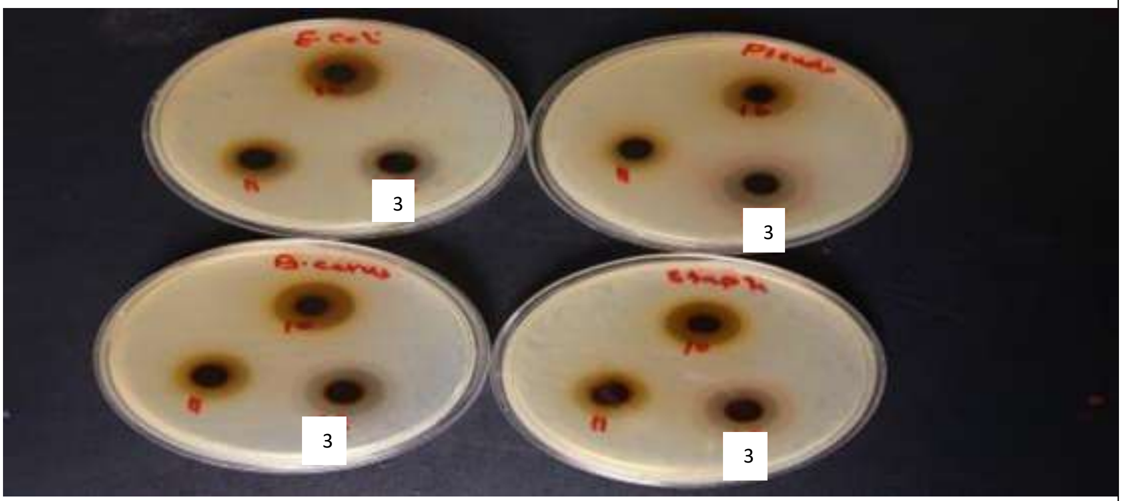

Fig (11): Zones of inhibition of antibacterial activity of(1) nanocurcumin, (2) [NCur/MnOF2eO3], (3) [NCur/CuOFe2O3] , and (4) [NCur/CuOFe2O3] nanocomposites on Pseudomonas aeruginosa(-), Bacillus cereus (+), Escherichia Coli (-) and Staphylococcus aureus(+)

Conclusions: The nanocomposites CuOFe2O3, MnOFe2O3 and ZnOFe2O3 /

curcumin particles were successfully synthesized by Eco-friendly hydrothermal method using (copper, nickel, and manganese) acetate and ferric chloride as a precursor, in addition the curcumin as a matrix.

The FTIR spectroscopic data indicated the composition of the metal oxides nanoparticles and the resulting data from SEM and XRD also indicated that the nanoparticles within the nanoscale and confirmed the nanocrystalline nature of the composite particles. Moreover, for all nanocomposites, energy dispersive X-ray diffraction spectroscopy (EDX) were recorded, where EDX-layered image and compositional maps provided more confirmation of CuOFe2O3, MnOFe2O3 and ZnOFe2O3 / curcumin and has been demonstrated success in forming spinel oxide with cubic crystallites phase, also the mean particle size calculated by the Debye-Scherrer formula (22.8-17.7 nm). In addition, the 3D surface images of the AFM of these nanostructures indicated the diffusion of the oxide nanoparticles on the surface of curcumin.

Curcumin nanocomposites showed positive activity and high efficacy against selected microbes and was the greatest effectiveness of nanocomposites [CuOFe2O3 / Curcumin].

Acknowledgement

The researchers express their great gratitude to the Department of Chemistry / and the Deanship of the College of Science / University of Baghdad for the material and moral support that enabled us to complete this research.

References

[1] Ullah, F.; Liang, A.; Rangel, A.; Gyengesi, E.; Niedermayer, G. High bioavailability curcumin: An anti-inflammatory and neurosupportive bioactive nutrient for neurodegenerative diseases characterized by chronic neuroinflammation.

Arch. Toxicol. **2017**, *91*, 1623–1634, doi:10.1007/s00204-017 1939-4.

[2] Jakubek, M.; Kejík, Z.; Kaplánek, R.; Hromádka, R.; Šandriková, V.; Sýkora, D.; Antonyová, V.; Urban, M.; Dytrych, P.; Mikula, I. Strategy for improved therapeutic efficiency of curcumin in the treatment of gastric cancer. *Biomed. Pharmacother.* **2019**, *118*, 109278.

[3] Grykiewicz, G.; Silfirski, P. Curucmin and curcuminoids in quest for medicinal status. *Acta Biochim. Pol.* **2012**, *59*, 201–212.

[4] Esatbeyoglu, T.; Huebbe, P.; Insa, M.A.; DawnChin, E.; Wagner, A.E.; Rimbach, G. Curcumin—From Molecule to Biological Function. *Angew. Chem. Int. Ed.* **2012**, *51*, 5308–5332.

[5] Gupta, S.; Prasad, S.; Ji, H.K.; Patchva, S.; Webb, L.J.; Priyadarsini, K.I.; Aggarwal, B.B. Multitargeting by curcumin as revealed by molecular interaction studies. *Nat. Prod. Rep.* **2011**, *28*,1937–1955.

[6] Priyadarsini, K.I. Chemical and structural features influencing the biological activity of curcumin. *Curr. Pharm. Des.* **2013**, *19*, 2093–2100.

[7] Carvalho, D. D. M., Takeuchi, K. P., Geraldine, R. M., Moura, C. J. De, & Torres, M. C. L. (2015). Production, solubility and antioxidant activity of curcumin nanosuspension. Food Science and Technology, 35(1), 115–119.

[8] Shengfeng Peng, Ziling Li ab, Liqiang Zou a, Wei Liu, Chengmei Liu , David Julian McClements.2017. Improving curcumin solubility and bioavailability by encapsulation in saponin-coated curcumin nanoparticles

prepared using a simple pH-driven loading method. DOI: 10.1039/C7FO01814B.

[9] F. Bai, J. Diao, Y. Wang, S. Sun, H. Zhang, Y. Liu, Y. Wang and J. Cao, Journal of agricultural and 615 food chemistry, 2017, **65**, 6840-6847.

[10] Zahra Naderi, Javad Azizian.,2018. Synthesis and characterization of carboxymethyl chitosan/Fe3O4 and MnFe2O4 nanocomposites hydrogels for loading and release of curcumin. Journal of Photochemistry & Photobiology, B: Biology 185 206–214.

[11] Maiti, P.; Dunbar, G.L. Use of Curcumin, a Natural Polyphenol for Targeting Molecular Pathways in Treating Age-Related Neurodegenerative Diseases. *Int. J. Mol. Sci.* **2018**, *19*, doi:10.3390/ijms19061637.

[12] Hamed Nosrati, Naser Sefidi, Ali Sharafi, Hossein Danafar, Hamidreza Kheiri Manjili.2018,. Bovine Serum Albumin (BSA) coated iron oxide magnetic nanoparticles as biocompatible carriers for curcumin-anticancer drug. Bioorganic Chemistry 76 , 501–509.

[13] D. Brahatheeswaran, A. Mathew, R. G. Aswathy, Y. Nagaoka, K. Venugopal, Y. Yoshida, T. Maekawa and D. Sakthikumar, Biomed. Mater., 2012, 7, 045001.

[14] Zoran Markovi , MáriaKová cová, Matej Mi cušík, Martin Danko, Helena Švajdlenková, Angela Kleinová, Petr Humpolí cek, Marián Lehocký, Biljana Todorovi Markovi, Zdeno Špitalský. 2018. Structural, mechanical, and antibacterial features ofcurcumin/polyurethane nanocomposites. DOI: 10.1002/app.47283

[15] Mangolim, C. S., Moriwaki, C., Nogueira, A. C., Sato, F., Baesso, M. L., & Neto, A. M. (2014). Curcumin-beta-cyclodextrin inclusion complex: Stability, solubility, characterisation by FT-IR, FT-Raman, X-ray diffraction and photoacoustic spectroscopy, and food application. Food Chemistry, 153, 361–370.

[16] M. Mumtaz a,b , S. Naeem a, K. Nadeem a, F. Naeem a, Abdul Jabbar a, Y.R. Zheng b,Nawazish A. Khan c, M. Imran d,.2013. Study of nano-sized $(ZnFe_2O_4)_y$ particles/CuTl-1223 superconductor composites. Solid State Sciences 22 ,21-26.

[17] Kyung-Won Jung, Seon Yong Lee, Young Jae Lee ,.2018. Facile one-pot hydrothermal synthesis of cubic spinel-type manganeseferrite/biochar composites for environmental remediation of heavy metals from aqueous solutions. Bioresource Technology 261 , 1–9.

[18] F. Shahbaz Tehrani · V. Daadmehr · A.T. Rezakhani · R. Hosseini Akbarnejad · S. Gholipour.2012. Structural, Magnetic, and Optical Properties of Zinc- and Copper-Substituted Nickel Ferrite Nanocrystals. J Supercond Nov Magn DOI 10.1007/s10948-012-1655-5.

[19] Fatemeh Ahmadi, Maryam Ghasemi-Kasman, Shahram Ghasemi, Maryam Gholamitabar Tabari, Roghayeh Pourbagher, Sohrab Kazemi, Ali Alinejad-Mir,.2017. Induction of apoptosis in HeLa cancer cells by an ultrasonic-mediated synthesis of curcumin-loaded chitosan–alginate–STPP nanoparticles. International Journal of Nanomedicine 8545–8556.

[20] Costa, A.C.F.M., Silva, V.J., Cornejo, D.R., Morelli, M.R., Kiminami, R.H.G.A., Gama, L.: Magnetic and structural properties of NiFe2O4 ferrite nanopowder doped with Zn2+. J. Magn. Magn. Mater. 320, e370 (2008).

[21] F. Shahbaz Tehrani · V. Daadmehr · A.T. Rezakhani · R. Hosseini Akbarnejad · S. Gholipour,.2012. Structural, Magnetic, and Optical Properties of Zinc- and Copper-Substituted Nickel Ferrite Nanocrystals. J Supercond Nov Magn DOI 10.1007/s10948-012-1655-5.

[22] S. Kimura, T. Mashino, T. Hiroki, D. Shigeoka, N. Sakai, L. Zhu, Y. Ichiyanagi, Effect of heat treatment on Jahn–Teller distortion and magnetization in Cu ferrite nanoparticles, Thermochim. Acta. 532 (2012) 119–122.

[23] 19.T. Tsoncheva, E. Manova, N. Velinov, D. Paneva, M. Popova, B. Kunev, K. Tenchev, I. Mitov, Thermally synthesized nanosized copper ferrites as catalysts for environment protection, Catal. Commun. 12 (2010) 105–109.

[24] Mobina Mahdavinasab, Mahshid Hamzehloueian, , Yaghoub Sarrafi ,.2019. Preparation and application of magnetic chitosan/graphene oxide composite supported copper as a recyclable heterogeneous nanocatalyst in the synthesis of triazoles. International Journal of Biological Macromolecules 138 , 764–772.

[25] Y. Fu, P. Xiong, H. Chen, X. Sun, X.Wang, High photocatalytic activity ofmagneticallyseparable manganese ferrite–graphene heteroarchitectures, Ind. Eng. Chem. Res. 51(2012) 725–731.

[26] Kaidi Wu, Yifan Luo1 , Ying Li and Chao Zhang,.

Synthesis and acetone sensing properties of ZnFe2O4/rGO gas sensors. Beilstein J. Nanotechnol. 2019, 10, 2516–2526.

[27] D.Shailendiran, N Pawar, A Chanchal, Pandey, R.P., H.B. Bohidar, A.K. Verma,. Characterization and Antimicrobial activity of Nanocurcumin and Curcumin.

[28] Anderson Clayton da Silvaa, Priscila Dayane de Freitas Santosa, Jéssica Thais do Prado Silvaa, Fernanda Vitória Leimanna, Lívia Brachtb, Odinei Hess Gonçalvesa,. Impact of curcumin nanoformulation on its antimicrobial activity. Trends in Food Science & Technology 72 (2018) 74–82.